https://doi.org/10.1016/j.biomaterials.2018.03.041

Second near-infrared emissive lanthanide complex for fast renal-clearable *in vivo* optical bioimaging and tiny tumor detection

Youbin Li, Xiaolong Li, Zhenluan Xue, Mingyang Jiang, Songjun Zeng, and Jianhua Hao**

Prof. S. J. Zeng, Y. B. Li, Z. L. Xue, X. L. Li, M. Y. Jiang

College of Physics and Information Science and Key Laboratory of Low-dimensional Quantum Structures and Quantum Control of the Ministry of Education, Synergetic Innovation Center for Quantum Effects and Applications, Hunan Normal University, Changsha, 410081, China.

E-mail: songjunz@hunnu.edu.cn

Prof. J. H. Hao

Department of Applied Physics and Materials Research Center, The Hong Kong Polytechnic University, Hong Kong.

E-mail: jh.hao@polyu.edu.hk

Keywords: molecule probe, NIR-II bioimaging, renal clearance, tiny tumor diagnosis, X-ray bioimaging.

Abstract:

In vivo optical imaging by using a new imaging window located at short-wavelength infrared region (1000-1700 nm, named as NIR-II) presents an unprecedented improvement in imaging sensitivity and spatial resolution over the traditional visible and near-infrared light. However, the most developed NIR-II-emitters are hardly excreted from live animals, leading to unknown long-term toxicity concerns, which hinder the widespread applications of this advanced imaging technology. Here, we developed a new generation molecular NIR-II-emitting probe based on Nd-diethylene triamine pentacetate acid (DTPA) complex. The designed molecular Nd-DTPA probe with bright narrow band emission at 1330 nm is successfully used for highly sensitive *in vivo* NIR-IIa bioimaging with rapid renal excretion and high biocompatibility and optical-guided tiny tumor (down to ~3 mm) detection for the first time. Moreover, the Nd-DPTA complex also holds great promise as an X-ray contrast agent. This findings open up the possibility for designing a new generation of multi-modal small molecular probe for early tumor diagnosis and favor the clinic translation of the advanced NIR-II imaging method.

1. Introduction

Noninvasive fluorescent imaging by using optical probe is one of the most important imaging technique for the early detection of disease owing to the cellular or molecular level information and high imaging sensitivity.[1] Although the traditional near infrared light (NIR-I, 650-900 nm) emitting optical probes with low tissue-absorption nature are well-developed for deep-tissue bioimaging, some performance parameters (penetration depth, imaging sensitive and resolution etc.) are still limited by the large scattering losses of NIR-I light.[2] Recent optical simulations demonstrate a new advanced optical transparent window with short wavelength infrared light (SWIR, NIR-II, 1000-1700 nm), which presents lower optical absorption and auto-fluorescence than NIR-I window, but up to 1000-fold reduction in scattering losses, subsequently resulting in unprecedented improvements in detection depth and imaging resolution.[1b,3] Therefore, developing the new advanced NIR-II optical probe with high emission intensity, large optical penetration depth in biotissue, and high biocompatibility is vital important for high sensitivity/resolution optical bioimaging.

In this context, some NIR-II optical probes capable of producing NIR-II emissions such as quantum dots (QDs)[4] and single-walled carbon nanotubes (SWNTs)[5] are emerging. However, most of the reported NIR-II-emitting QDs comprise the toxic elements such as lead or mercury, making them unsuitable for bioapplications.[1b] Single-walled carbon nanotubes (SWNTs) have demonstrated good performance in *in vivo* applications.[5] However, SWNTs still face significant challenges including low emission intensity, broad emission peaks (band width: > 300 nm), and large size distributions, making them unattainable for the size-dependent biological barriers study.[1b,6] Recently, rare earth based nanoparticles with well controlled size and narrow-band emission were emerged as promising probes for NIR-II bioimaging owing to their advantages of high efficiency, low photo-bleaching and long luminescence lifetimes.[1b,7] However, most of the designed rare earth-based probes usually present unspecific liver/spleen uptake and are excreted slowly from live animals, leading to

unknown long-term toxicity concerns, which remarkably limited their widespread application in NIR-II bioimaging. As it is well known that the ability of rapid excretion of imaging contrast agent is vital for clinical use. Recently, Dai's group demonstrated a pioneering study of designing small organic molecular probes with 1000 nm emission for NIR-II imaging.[8] However, these small molecular probes still presented the broad-band emission and relative low photostability(>10% photobleaching degree in 1 h)[8b], which inhibited the practice use of nonoverlapping signals for multispectral imaging. Therefore, it is appealing to design novel NIR-II imaging agent with narrow-band and bright NIR-II emission, rapid excretion, high biocompatibility for eventually overcoming the barrier of clinical use.

Herein, we design a new type of molecular Nd-based complex (Nd-DTPA) with efficient narrow band NIR-IIa emission centered at 1330 nm (band width: ~ 65 nm), high biocompatibility, and rapid excretion from the kidney. The NIR-IIa emitting Nd-DTPA probe was successfully used as *in vivo* tracking. More importantly, the optical-guided tiny tumor (< 3 mm) detection was demonstrated by using the designed Nd-DTPA probe for the first time. Apart from the excellent NIR-IIa bioimaging nature, the designed Nd-DTPA can also be used as X-ray imaging agent owing to the large X-ray absorption coefficient of Nd element.[9]

2. Results and Discussion

2.1. Synthesis and NIR-II emitting property

The Nd-DTPA was primarily synthesized through a chelation of the Nd^{3+} and DTPA, as presented in **Scheme 1.** The N-Methyl-D-glucamine was added into the Nd-DTPA solution to tune the pH value to 7.2. The surface ligands of the precursor and Nd-DTPA were analyzed by Fourier-transform infrared (FTIR) spectroscopy (**Fig. 1a)**. As demonstrated, for pure DTPA, the peaks at 1733 cm^{-1}, 1700 cm^{-1}, and 1634 cm^{-1} are ascribed to the stretching vibration of C=O (-COOH), C=O (-CONH-), and the deformation vibrations of N-H (-CONH-), respectively. While in Nd-DTPA sample, the stretching and deformation vibration bands of 1733/1700/1634 cm^{-1} were disappeared and a new vibration peaks at 1595 cm^{-1} was

observed and ascribed to the vibration of O-C-O (carboxylate), unambiguously validating the coordination of COO^- with Nd^{3+}.[10] The ultraviolet (UV)-vis absorption spectrum of the Nd-DTPA solution in water presented several sharp absorption peaks of Nd^{3+} centered at 741 nm ($^4I_{9/2}—^4F_{7/2}$), 801 nm ($^4I_{9/2}—^4F_{5/2}$) and 872 nm ($^4I_{9/2}—^4F_{3/2}$), indicating an excellent absorption of NIR light of about 800 nm (Fig. 1b). To reveal the NIR-II emitting properties, the NIR emission spectrum of Nd-DTPA was detected under the excitation of 808 nm laser. As shown in Fig. 1b and 1c, the Nd-DTPA presents the efficient NIR-II emissions centered at 1050 nm (band width: ~ 45 nm) and 1330 nm (band width: ~ 65 nm), which can be ascribed to the electronic transitions $^4F_{3/2}—^4I_{11/2}$ (1050 nm), and $^4F_{3/2}—^4I_{13/2}$ (1330 nm) of Nd^{3+}, respectively. It is noted that the photo-stability is a key characteristic for molecular optical probes. Therefore, the photo-stability of Nd-DTPA molecule was tested with a continuous 808 nm laser excitation for 1 h at 1 w cm^{-2} (Fig. 1d). The photo-stability curve (Fig. 1e) and *in vitro* phantom bioimaging (**Supplementary Fig. S1)** reveal the designed Nd-DTPA present superior photo-stability with photobleaching degree of 3.4% in 1 h, which is relatively lower than the previous report[8b]. These results suggest that the Nd-DTPA possesses remarkable narrow band emission in NIR-II region (1050/1330 nm) and superior photo-stability, making it an ideal agent for NIR-II bioimaging with high photostability.

2.2. *In vivo* NIR-IIa bioimaging

Prior to using Nd-DTPA for *in vivo* imaging, the cell toxicity of this designed molecular Nd-DTPA probe was evaluated via a 3-(4, 5-dimethylthiazol-2-yl)-2, 5-diphenyl-tetrazolium bromide (MTT) method (**Supplementary Fig. S2**). As demonstrated, the cell viability of Nd-DTPA in HeLa cells was 99% when treated with 100 μg mL^{-1} of Nd-DTPA. When further increasing the concentration of Nd-DTPA to 1000 μg mL^{-1}, the cell viability was still remained at 90%, indicating the very low cell toxicity of the Nd-DTPA molecules. Encouraged by the low cytotoxicity and strong 1050 nm emission, we first performed *in vivo* NIR-II bioimaging by detecting the 1050 nm emission via a home-made NIR-II imaging

system (**Supplementary Fig. S3)** installed with a fiber-coupled 808 nm laser as light source. As shown in **Fig. 2c and 2d**, an obvious NIR-II signal of mouse food was observed by using a 1000-1100 nm band-pass filter, while, the signal intensity of mouse food was almost disappeared by detecting the 1330 nm emission, indicating the efficiently diminishing the undesired interference signal caused by mouse food. Further *in vivo* bioimaging (Fig. 2e and 2f**)** also demonstrated that the undesired signal of stomach caused by mouse food was fully removed by measuring the 1330 nm emission via a band-pass filter (1200-1400 nm). It should be noted that imaging in the NIR-IIa window (1300 -1400 nm) can greatly minimize the scatter of rejection photons below 1300 nm, and avoid the light absorption from water vibration over 1400 nm.[8c] Based on the above analysis, our designed Nd-DTPA probe presents efficient NIR-IIa emission located at 1330 nm, which is beneficial for bioimaging applications. Then, *in vivo* NIR-IIa bioimaging of a Kunming mouse was performed by intravenous injection of Nd-DTPA. As demonstrated in **Fig. 3a**, within a few second, a significant fluorescence signal in kidney was observed and the fluorescence signal in the kidney was gradually enhanced after 25 min injection and then tended to slight decrease after 35 min. The optical signal was finally disappeared within 120 min, indicting the rapidly excretion of the Nd-DTPA probe from the kidneys. In addition, NIR-IIa bioimaging of the supine positioned mouse was performed for further proof of the *in vivo* excretion mechanism of the Nd-DTPA molecules. As illustrated in Fig. 3b, strongsignal was observed in bladder within 10 min, implying the rapid excretion rate of the Nd-DTPA probe from the kidney and vessels to the bladder. Moreover, the Nd-DTPA probe was fully excreted from the bladder within 11 h, indicating the fast renal clearance of the Nd-DTPA molecule. The urine sample collected after 2 h in jection also showed a strong fluorescence signal, which further proved the renal clearance and high stability of Nd-DTPA *in vivo*. These findings reveal that the Nd-DTPA with efficient emission at 1330 nm is an ideal probe for NIR-IIa bioimaging with deep tissue penetration, low cytotoxicity and rapid excretion, paving the way for designing the new

type of NIR-IIa imaging agent and favoring the clinical translation of NIR-II imaging technology.

2.3. NIR-IIa imaging-guided tiny tumor detection.

In vivo highly sensitive tiny tumor detection has played a key role for early cancer diagnosis. However, tiny tumor (below 5 mm) detection was limited by the lower uptake of macro molecules drugs and dramatic comparable geometric resistances.[11] Therefore, designing of nanoprobes with molecular functionality to be accumulated in the tumor site is a crucial step. Compared to the traditional QDs and rare earth nanomaterials, the Nd-DTPA small molecule agents present a smaller size and excellent pharmacokinetics, making it efficient accumulation in the tumor site, as well as rapid excretion from living animals. Therefore, *in vivo* tiny tumor detection was performed by intravenous injection of 125 μL Nd-DTPA solution. As shown in **Fig. 4a**, after 60 s injection, obvious NIR-IIa signal can be detected from the kidney and tumor site, indicating the NIR-IIa bioimaging based on Nd-DTPA molecule can afford the pinpointing location of tumor. The NIR-IIa fluorescence signal in the tumor site becomes distinguishable over time and is slightly decreased after 20 min injection, revealing an ultra-sensitivity detection of tumor. The accumulation of Nd-DTPA in the tumor site is mainly ascribed to the enhanced permeation and retention (EPR) effect of tumor. To further demonstrate the ultrasensitive detection of tiny tumor, *ex-vivo* NIR-IIa imaging of the dissected tumor was performed. As demonstrated in Fig. 4c, strong signal was observed in the tumor site, further validating the accumulation of Nd-DTPA in tumor site. In addition, we further analyzed time-dependent intensity change and maximal signal in the kidney and tumor site, as shown in Fig. 4d and 4e. The maximal signal intensity in the tumor site exhibit comparable intensity to that in kidney, demonstrating the efficient uptake of Nd-DTPA in tumor. By putting together, we conclude that the designed Nd-DTPA molecule should be a suitable NIR-II agent to achieve highly sensitive optical-guided tiny tumor diagnosis.

2.4. *In vivo* X-ray bioimaging

Recently, X-ray imaging has triggered considerable interests in diagnostic medicine owing to its deep tissue penetration and high resolution.[9] However, as X-ray imaging contrast agents, elements with high atomic number (high-Z), high biocompatibility and acceptable safety profiles are urgently needed.[9b] Currently, small iodinated molecules with effectively absorbed X-ray nature are used as X-ray contrast agent in clinical applications. Compared with the I-based X-ray imaging agent, the Nd-based molecular probe may have superior X-ray imaging contrast because of the larger atomic number and K-edge value of Nd (43.5 keV) than I (33 keV).[12] Therefore, apart from the excellent NIR-IIa imaging, the designed Nd-DTPA can also be used as promising agent for X-ray bioimaging owing to the large K-edge value (43.5 keV). To validate this, X-ray imaging based on Nd-DTPA and iobitridol was performed. As shown in **Fig. 5b and 5c,** the *in vitro* phantom images of both agents exhibit obvious X-ray absorption enhancement when increasing their concentration. Moreover, the Nd-based agent presents a higher X-ray absorption contrast than that of I at identical concentration. Hounsfield units (HU) values of Nd-DTPA and iobitridol were further tested. As demonstrated in Fig. 5d, the HU values of both agents increased linearly when increasing the concentration. More importantly, a higher HU value of Nd-DTPA was detected at an equivalent concentration. These results illustrate that our designed Nd-DTPA possesses superior X-ray imaging efficacy than that of I-based agent. We further carried out the *in vivo* X-ray bioimaging of a Kunming mouse (the left panel of Fig. 5e) without injection and with subcutaneous injection (the right panel of Fig.5e) of Nd-DTPA probe by using an *in vivo* imaging system (Bruker *In Vivo* FX Pro). As illustrated by the blue-dotted circles in Fig. 4e, the injection site exhibits high X-ray absorption contrast. However, no obvious signal is observed in the control mouse, revealing that the Nd-based contrast agent is an ideal probe for *in vivo* X-ray bioimaging.

2.5. Histological analysis

To evaluating the long-term *in vivo* toxicity, histological assessment based on Nd-DTPA was performed. As shown in **Fig. 6**, the mice were dissected in terms of the heart, liver, spleen, lung and kidney at 3 and 7 days after intravenously injected with Nd-DTPA. No tissue damage or any other signal of inflammatory lesion was observed, implying the high biocompatibility and low toxicity of the Nd-DTPA molecule.

3. Conclusion

In conclusion, we have developed a new type of Nd-DTPA molecule probe with fast excretion for NIR-IIa bioimaging, which is an important counterpart of Gd-DTPA (a highly biocompatible magnetic resonance imaging agent for clinical use approved by the US Food and Drug Administration, FDA). Our designed Nd-DTPA possesses high photostability and narrow-band NIR-IIa emission at 1330 nm. By combining bright narrow-band NIR-II emission and excellent biocompatibility, optical bioimaging-guided tiny tumor (down to ~3 mm) detection was successfully demonstrated for the first time. Except the excellent optical properties, the Nd-DTPA was also used for *in vivo* molecule X-ray imaging agent. These findings pave the way of designing a new dual-modal molecular probe for synergetic NIR-II and X-ray bioimaging for highly sensitive tiny tumor (~ 3 mm) detection and promote the clinical translation of the next generation optical imaging technology by using NIR-II region.

4. Experimental Section

Chemicals and materials: All chemical reagents were obtained from the commercial supply and used without further purification. Rare earth $NdCl_3 \bullet 6H_2O$ (99.99%) was purchased from QingDa elaborate Chemical Reagent Co. Ltd (Shandong). Diethylene triamine pentacetate acid (DTPA) and N-Methyl-D-glutamines were obtained from the ScienMax.

Synthesis of Nd-DTPA: For synthesis of the Nd-based complex, 15 ml water in the beaker was heated to 50 C, then 1.1 mmol DTPA was added into the water and kept stirring for 20

min. 1 mmol $NdCl_3$ solution (1 M) was then added and stirred until forming a transparent solution. The obtained Nd-DTPA solution was treated with N-Methyl-D-glutamines to adjust the pH value to 7.2.

Cytotoxicity assay: To evaluate the cell viability of Nd-DTPA, the viability of HeLa cells based on MTT proliferation assay method was evaluated. In a typical process, HeLa cells in a 96-well micro plate (6000 cells per well) were kept at 37 C under 5% CO_2. Then the cell culture medium in each well was replaced by Dulbecco's Modified Eagle Medium (DMEM) solution including 10% fetal bovine serum, 1% penicillin and streptomycin. The prepared Nd-DTPA solutions with different concentrations (0, 100, 200, 500, 1000 μL/mL) were added at 37 °C and with 5% CO_2 for 24 h. Finally, we measured the cell viability by using a typical MTT assay.

Characterization: The photoluminescent spectrum of Nd-DTPA was detected with a NIR-II spectroscopy (NIRQuest512, Ocean Optics). The 808 nm laser was used as an excitation light source at room temperature. UV-Vis absorption spectrum of Nd-DTPA in water solution was detected by using a Spectrophotometer system (UV-1800, Hunan Sino-Jewell Electronics Co.Ltd.). The surface ligands of Nd-DTPA were analyzed via a Fourier transform infrared spectrum (FTIR) by using a Magna 760 spectrometer (Nicolet).

NIR-IIa optical bioimaging: A home-made small animal NIR-II bioimaging system equipped with a thermoelectric cooled InGaAs camera (Model: NIRvana^{TM} Camera System, operating temperature: -80 C , Princeton Instruments) and fiber-coupled 808/980 lasers (**Supplementary Fig. S3)** was used for NIR-II bioimaging. The fluorescence signal was collected by using the system installed with 808 nm diode laser as light source and filtered by a (1200-1400 nm) band pass filter. For *in vivo* bioimaging, a Kunming mouse was intraperitoneally injected with pentobarbital sodium aqueous (150 μL/10 wt%). Then Nd-DTPA (125 μL) was injected into the mouse by intravenous injection at tail vein. Finally, the

fluorescence signal was collected by using the system under an excitation powder density of 100 mW/cm^2. All animal procedures comply with the institutional animal use and care regulations approved by the Laboratory Animal Center of Hunan Province.

NIR-IIa optical bioimaging of tiny tumor detection: The tumor-bearing mouse model was achieved by subcutaneous injection of 8×10^6 MAT-Ly-Lu-B-2 (Mat) cells into a BALB/C mouse. We then carried out the *in vivo* tumor detection after inoculation for 3 days when the tumor size reached about ~3 mm. Firstly, 150 μL of pentobarbital sodium aqueous solution (10 wt%) was intraperitoneally injected into the inoculated tumor mouse to anesthetize it. 125 μL of Nd-DTPA solution was then injected into the mouse by intravenous injection. The fluorescence signal was captured at different period times by using the same bioimaging system equipped with 808 nm laser as light source. The emission filter was set as 1330 nm, and the exposure time was set as 2000 ms. *Ex-vivo* bioimaging of the tumor was executed by the same parameters. The digital picture of the tumor was taken by using a Canon digital camera.

In vivo and in vitro X-ray bioimaging: To demonstrate the feasibility of the as prepared Nd-DTPA molecules for *in vivo* X-ray bioimaging, a Kunming mouse was first anesthetized. And 125 μL of Nd-DTPA with concentration of 30 mg/mL was subcutaneously injected into the mouse. Then X-ray bioimaging was tested via an *in vivo* imaging system (Bruker *In Vivo* FX Pro). To assess the X-ray contrast efficacy, Nd-DTPA and Iobitridol were dispersed in water with different Nd and I concentrations over the range from 0 to 60 mg/mL, respectively. *In vitro* phantom X-ray imaging based on these agents was collected. *In vivo* X-ray imaging was executed with the following parameters: voltage, 45 kVp; aluminium filter, 4 mm; and exposure time, 30 s.

Histology analysis: For histology analysis, Kunming mice were sacrificed at 3 and 7 day after intravenously injected with 125 μL of Nd-DTPA solution. Major organs including heart, liver,

spleen, lung, and kidney were isolated from the mice. Then the tissue sections were stained with hematoxylin and eosin (H&E) and visualized by using an optical microscope.

Supporting Information

Supporting Information is available from the Wiley Online Library or from the author.

Acknowledgements
This work was supported by the National Natural Science Foundation of China (No. 21671064), specialized research Fund for the Doctoral Program of Higher Education of China (No. 20114301120006), Scientific Research Fund of Hunan Provincial Education Department (13B062), and the Hunan Provincial Innovation Foundation for Postgraduate (CX2017B223).

Received: ((will be filled in by the editorial staff))
Revised: ((will be filled in by the editorial staff))
Published online: ((will be filled in by the editorial staff))

[1] a) R. Weissleder, M. J. Pittet, *Nature* **2008**, 452, 580-589; b) D. J. Naczynski, M. C. Tan, M. Zevon, B. Wall, J. Kohl, A. Kulesa, S. Chen, C. M. Roth, R. E. Riman & P. V. Moghe, *Nat. Commun.* **2013**, 4, 2199.

[2] a) S. Y. Han, R. R. Deng, X. J. Xie, X. G. Liu, J. Zhou, *Angew. Chem. Int. Ed*. **2014**, 53, 11702-11715; b) J. Zhou, Z. Liu, F. Y. Li, *Chem. Soc. Rev*. **2012**, 41, 1323-1349; c) S. L. Gai, C. X. Li, P. P. Yang, J. Lin, *Chem. Rev*. **2014**, 114, 2343-2389; d) X. M. Li, F. Zhang, D. Y. Zhao, *Chem. Soc. Rev*. **2012**, 44, 1346-1378; e) G. Y. Chen, C. H. Yang, P. N. Prasad, *Acc. Chem. Res*. **2013**, 46, 1474-1486; f) S. J. Zeng, Z. G. Yi, W. Lu, C. Qian, H. B. Wang, L. Rao, T. M. Zeng, H. R. Liu, H. J. Liu, B. Fei, J. H. Hao, *Adv. Funct. Mater.* **2014**, 26, 4051-4059; g) Z. G. Yi, X. L. Li, Z. L. Xue, X. Liang, W. Lu, H. Peng, H. R. Liu, S. J. Zeng, and J. H. Hao, *Adv. Funct. Mater.* **2015**, 25, 7119-7129; h) V. Pansare, S. Hejazi, W. Faenza, R. K. Prudhomme, *Chem. Mater.* **2012**, 24, 812-827; i) E. I. Alt noglu, J. H. Adair, *WIREs Nanomedicine and Nanobiotechnology* **2010**, 2, 461-477.

[3] Y. T. Lim, S. Kim, A. Nakayama, N. E. Stott, M. G. Bawendi, J. V. Frangioni, *Mol. Imaging.* **2003**, 2, 50-64.

[4] a) G. S. Hong, J. T. Robinson, Y. J. Zhang, S. Diao, A. L. Antaris, Q. B. Antaris, H. J. Dai, *Angew. Chem. Int. Ed*. **2012**, 51, 9818-9821; b) Y. Zhang, G. Hong, Y. Zhang, G. Chen, F. Li, H. J. Dai, Q. Wang, *ACS Nano* **2012**, 6, 3695-3702; c) J. Chen, Y. F. Kong, H. W. Fang, Y. Wo, D. J. Zhou, Z. Y. Wu, Y. X. Li, S. Y. Chen, *Chem. Commun.* ***2016***, 52, 4025-4028; d) B. H. Dong, C. Y. Li, , C. C. , Y. J. Zhang, Y. Zhang, M. J. Deng, Q. B. Wang, *Chem. Mater.* **2013**, 25, 2503-2509.

[5] a) K. Welsher, Z. Liu, S. P. Sherlock, J. T. Robinson, Z. Chen, D. Daranciang, H. J. Dai, *Nat. Nanotechnol.* **2009**, 4, 773-780; b) J. T., Welsher, K. Welsher, S. M. Tabakman, S. P. Wang, H. Sherlock, R. Luong, H. J. Dai, *Nano Res*. **2010**, 3, 779-793; c) K. Welsher, S. P. Sherlock, H. J. Dai, *Proc. Natl. Acad. Sci. USA.* **2011**, 108, 8943-8948; d) H. Yi, D. Ghosh, M. H. Ham, J. Qi, P. W. Barone, M. S. Strano, A. M. Belcher, *Nano Lett*. **2012**, 12, 1176-1183; e) J. T. Robinson, G. Hong, Y. Liang, B. Zhang, O. K. Yaghi, H. Yaghi, *J. Am. Chem. Soc.* **2012**, 134, 10664-10669; f) S. Diao, G. S. Hong, Robinson, J. T. Robinson, L. Y. Jiao, A. L. Antaris, J. Z. Wu, C. L. Choi, H. J. Dai, *J. Am. Chem. Soc.* **2012**, 134, 16971-16974; g) G. S. Hong, J. C. Lee, J. T. Robinson, U. Raaz, L. Xie, N. F. Huang, J. P. Cooke & H. J. Dai *Nat. Med.* **2012**, 18, 1841-1846; h) A. L. Antaris, J. T. Robinson, O. K. Yaghi, G. Hong, S. Diao, R. Luong, H. J. Dai, *ACS Nano* **2013**, 7, 3644-3652.

[6] S. D. Perrault, C. Walkey, T. Jennings, H. C. Fischer & W. C. W. Chan, *Nano Lett.* **2009**, 9, 1909-1915.

[7] a) I. Villa, A. Vedda, I. X. Cantarelli et al. *Nano Res*. **2015**, 8, 649-665; b) W. Rui, X. M. Li, L. Zhou, F. Zhang, *Angew. Chem. Int. Ed.* **2014**, 53, 1-6; c) M. Kamimura, T. Matsumoto, S. Suyari, M. Umezawaab, M. SogaRatiometric, *J. Mater. Chem. B* **2017**, 5, 1917-1925; d) X. Y. Jiang, C. Cao, W. Feng, F. Y. Li, *J. Mater. Chem. B* **2016**, 4, 87-95.

[8] a) Z. M. Tao, G. S. Hong, C. S. Ji, C. X. Chen, S. Diao, A. L. Antaris, B. Zhang, Y. P. Zhou, H. J. Dai, *Angew. Chem. Int. Ed.* **2013**, 52, 13002-13006；b) G. S. Hong, Y. P. Zou, A. L. Antaris, S. Diao, D. Wu, K. Cheng, X. D. Zhang, X. Chen, B. Liu, Y. H. He, J. Z. Wu, J. Yuan, B. Zhang, Z. M. Tao, C. Fukunaga & H. J. Dai, *Nat. Commun.* **2014**, 5 4206；c) G. S. Hong, S. Diao, J. L. Chang, A. L. Chang, C. X. Chen, B. Zhang, S. Zhao, D. N. Atochin, P. L. Huang, K. I. Andreasson, C. J. Kuo & H. J. Dai, *Nature Photonics.* **2014**, 8, 723-730; d) A. L. Antaris, H. Chen, S. Diao, Z. R. Ma, Z. Zhang, S. J. Zhu, J. Wang, A. X. Lozano, Q. L. Fan, L. L. Chew, M. Zhu, K. Cheng, X. C. Hong, H. J. Dai and Z. Cheng, *Nat. Commun.* **2017**, 8, 15269. e) A. L. Antairs, H. Chen, K. Cheng, Y. Sun, G. S. Hong, C. R. Qu, S. Qu, Z. X. Deng, X. M. Hu, B. Zhang, X. D. Zhang, O. K. , Z. R. Alampara H. J. Dai, *Nature Materials* **2016**, 15, 235-242.mbil, X. C. Hong, Z. Cheng,

[9] a) Y. L. Liu, K. L. Ai, J. H. Liu, Q. H. Yuan, Y. Y. He, L. H. Lu, *Angew. Chem. Int. Ed.* **2012**, 51, 1437-1442; b) S. B. Yu, A. D. Watson, *Chem. Rev.* **1999**, 99, 2353-2377.

[10] Z. P. Xu, Kurniawan, N. D. Kurniawan, P. F. Bartlett, and G. Lu, *Chem. Eur. J.* **2007**, 13, 2824-2830.

[11] C. Y. Liu, Z. Y. Gao, J. F. Zeng, Y. Hou, F. Fang, Y. L. Li, R. R. Qiao, L. Shen, H. Lei, W. S. Yang, M. Y. Gao, *ACS Nano* **2013**, 7, 7227-7240.

[12] http://physics.nist.gov/PhysRefData/XrayMassCoef/.

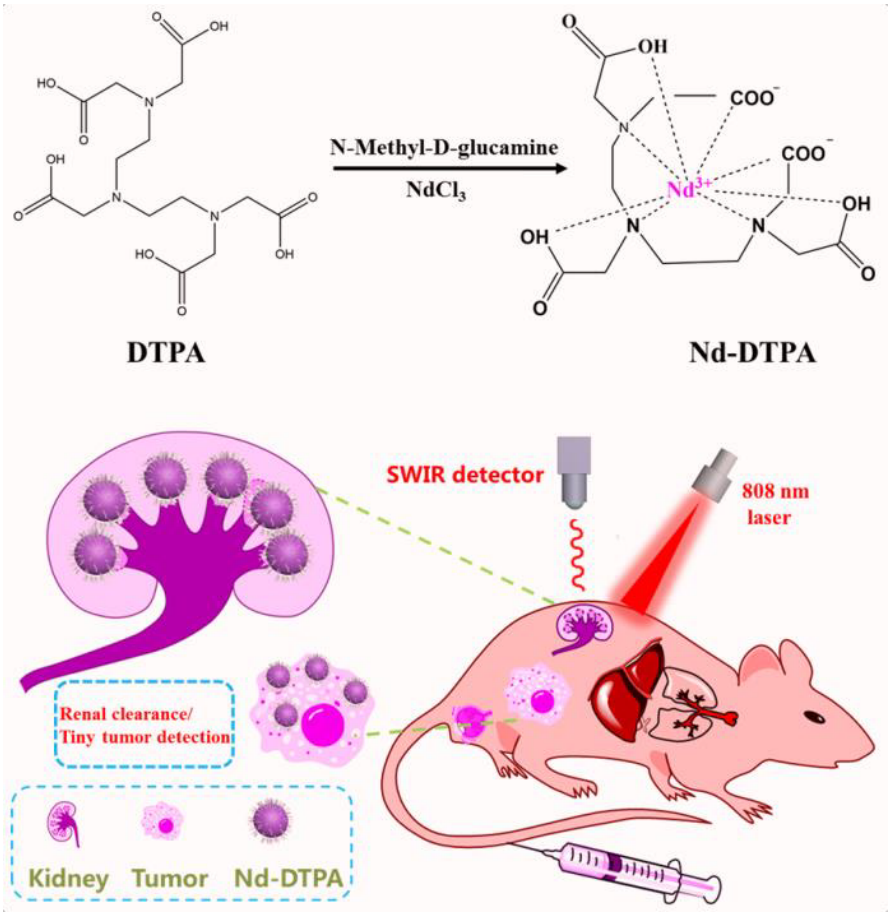

Scheme 1. Schematic illustration of the molecular structure of the DTPA and Nd-DTPA, along with the synthesis process of Nd-DTPA and bio-application process in NIR-IIa window under the 808 nm excitation.

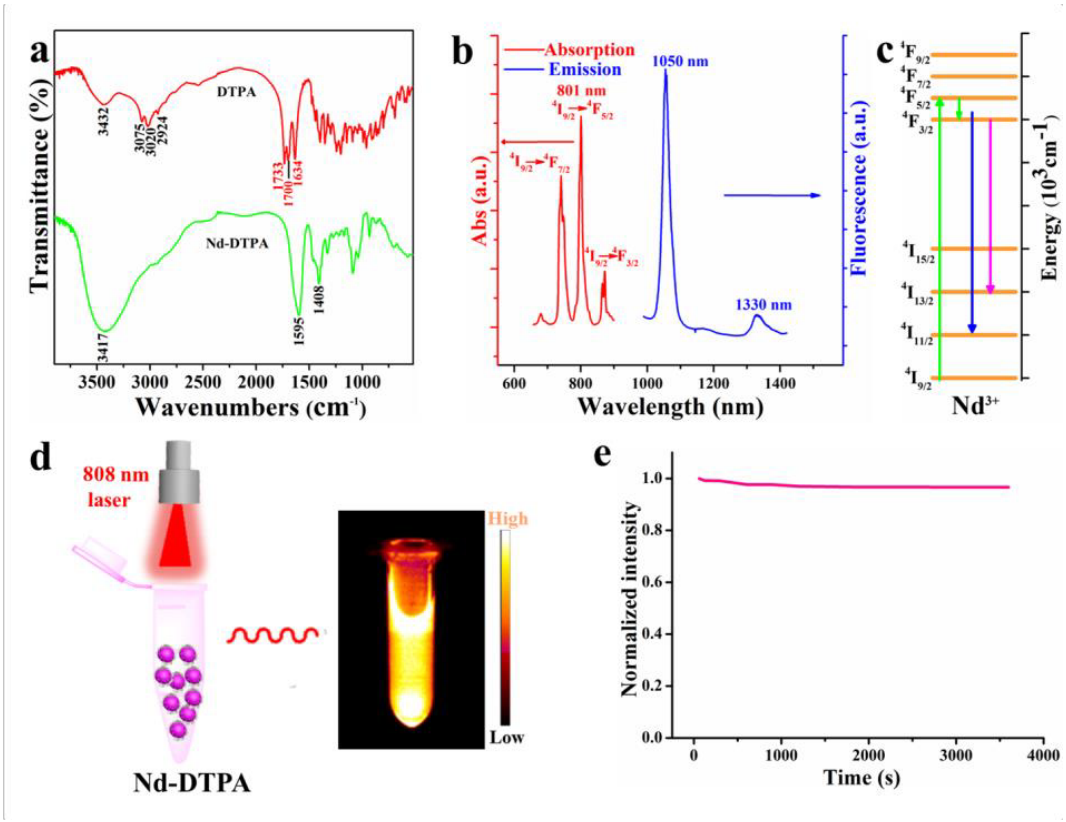

Figure 1. (a) FTIR spectra of Nd-DTPA and pure DTPA samples. (b) UV-vis absorption spectra (600-900 nm) and photoluminescent spectrum of the Nd-DTPA complex under the excitation of 808 nm laser, demonstrating the efficient narrow-band emissions centered at 1050 and 1330 nm. (c) Simplified energy level diagram. (d) A schematic diagram for the detection of the photostability. (e) Photostability curve of Nd-DTPA in water under continuous 808 nm illumination with power density of 1 w cm^{-2}, indicating the high photostability of the Nd-DTPA even for 3600 s.

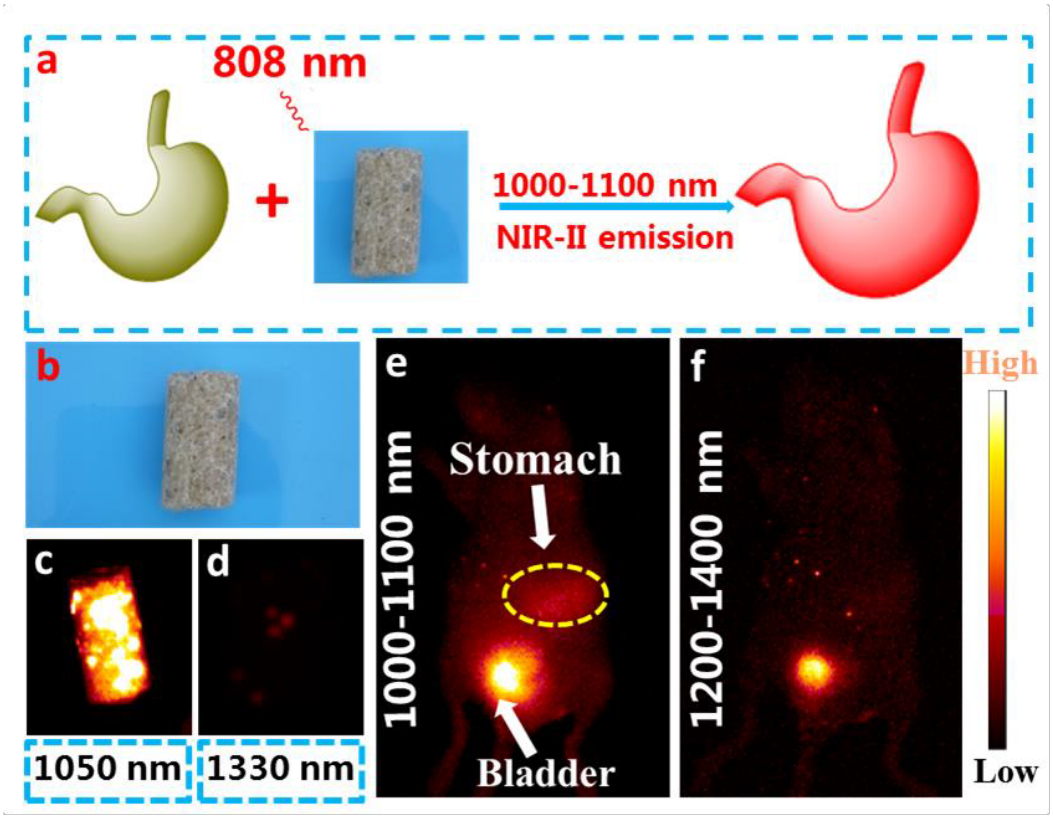

Figure 2. (**a**) A schematic diagram of demonstrating the bright NIR-II emission (1000-1100 nm) from the mouse food in stomach under the excitation of 808 nm laser. (**b**) Digital photo of the food. (**c**) and (**d**) The *in vitro* imaging of mouse food with different band pass filters. *In vivo* NIR-II imaging of a mouse via intravenous injection of Nd-DTPA by using a 1000-1100 nm band pass filter (**e**) and 1200-1400 nm band pass filter **(f)**. Fluorescence interference signal from stomach was obviously detected in (**e**) by using a 1000-1100 nm band pass filter.

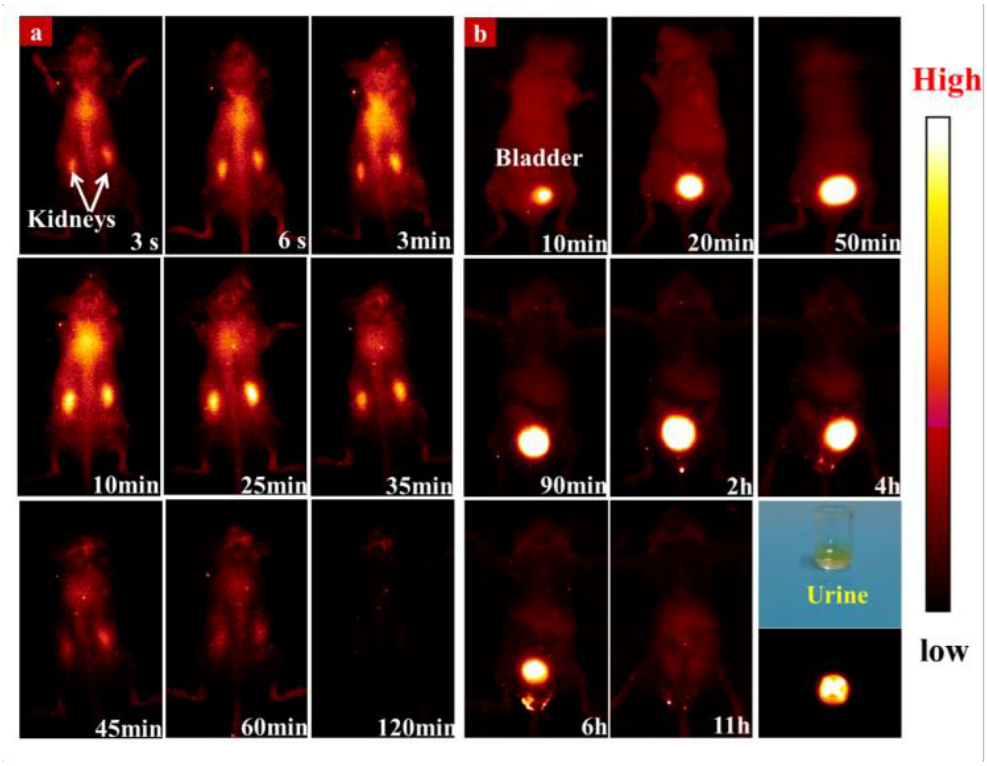

Figure 3. (a) *In vivo* NIR-IIa imaging of a mouse after intravenously injected with 125 μL Nd-DTPA solution. The prone positioned mouse was used to collect the kidney signals at various periods. (b) NIR-IIa imaging of the same mouse in the supine position, revealing the rapid excretion of Nd-DTPA molecule via kidney. The lower right corner denotes the NIR-IIa imaging of the urine sample (digital photograph in the lower right corner) collected after 2 h injection.

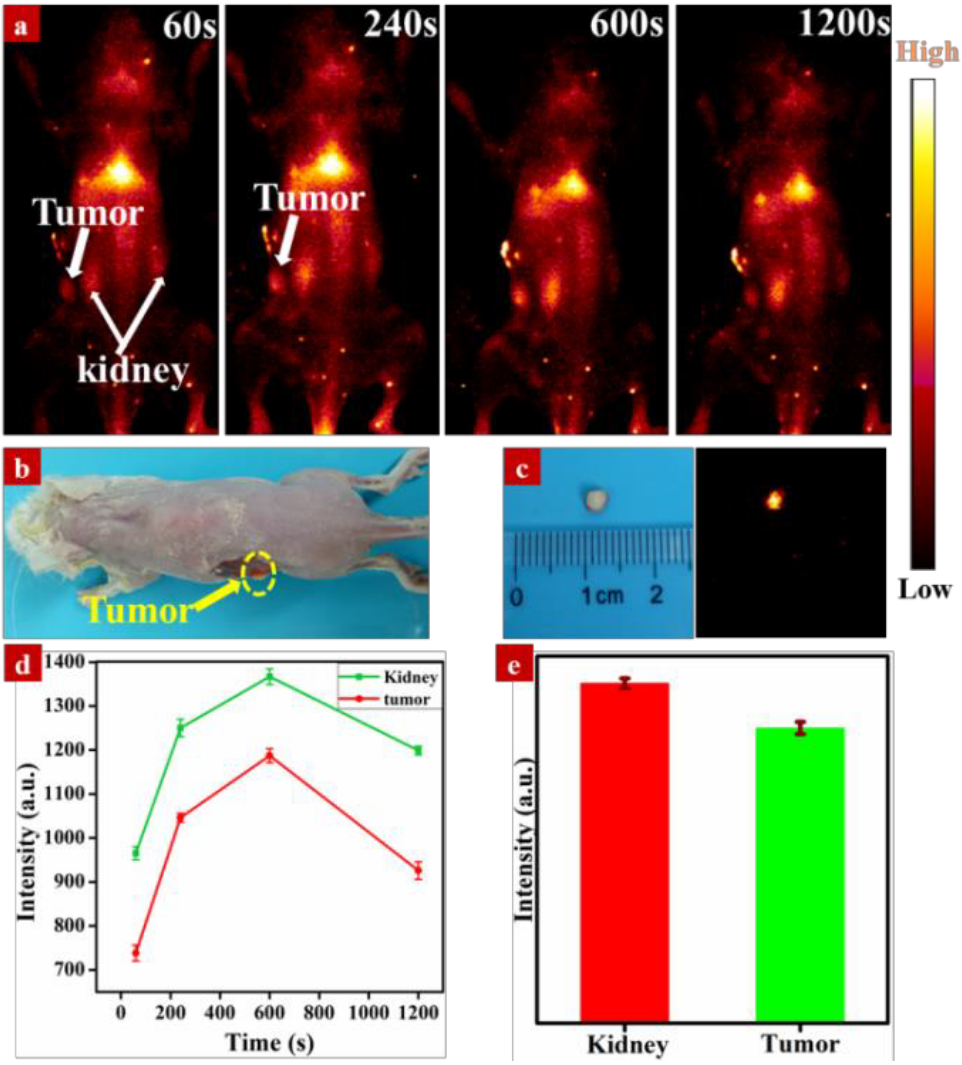

Figure 4. (a) NIR-IIa bioimaging of MAT-Ly-Lu-B-2 (Mat) cells tumor-bearing mouse after intravenously injected Nd-DTPA molecules at different periods. (b) In situ digital photography of the tumor-bearing mouse. (c) The digital photography of the tumor (left panel) and *ex vivo* NIR-IIa bioimaging (right panel), indicating the obvious fluorescence signal in the tumor site. (d) The time-dependent intensity changes of the kidney and tumor. (e) The maximal signal intensity in the kidney and tumor site.

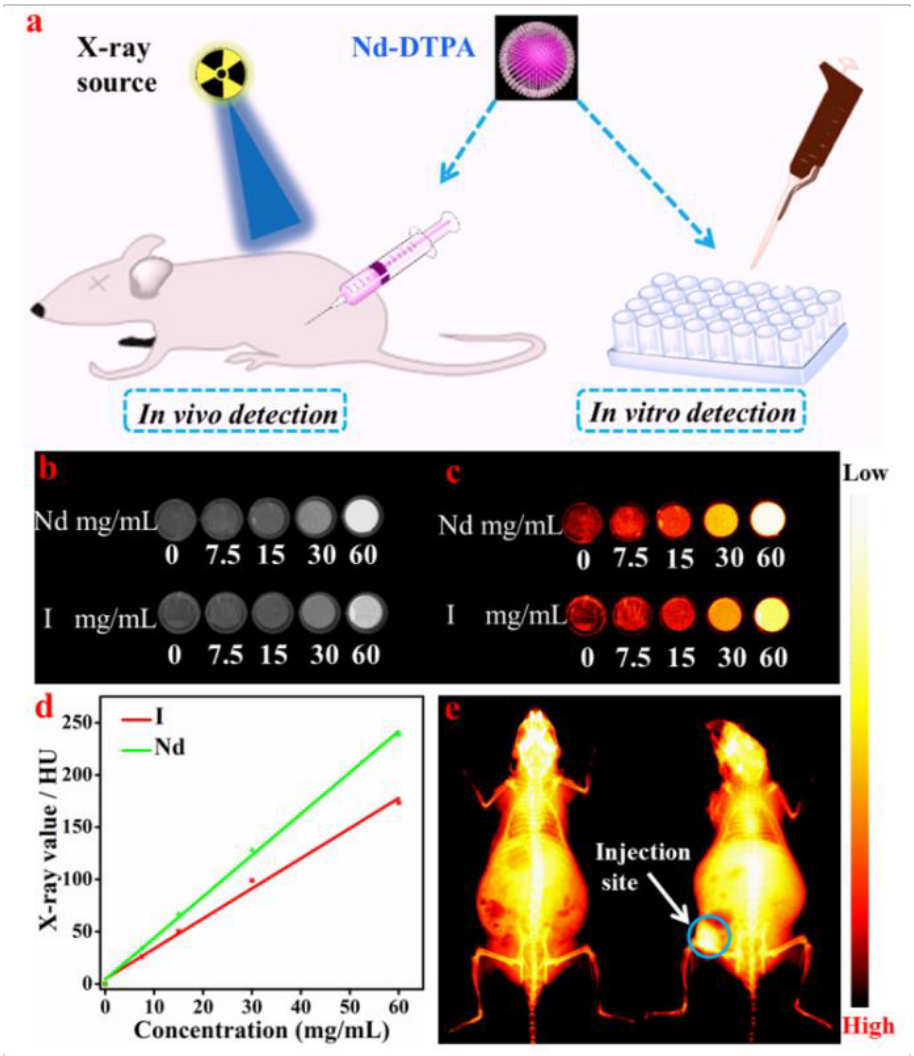

Figure 5. (**a**) A Schematic illustration of *in vivo* and *in vitro* X-ray imaging. (**b**) *In vitro* X-ray imaging of Nd-DTPA and iobitridol solution with different concentrations of Nd and I, respectively. (**c**) The corresponding pseudo-color images of (**b**). (**d**) X-ray absorption Hounsfield units (HU) value of Nd-DTPA (green lines) and iobitridol (red lines) as a function of the concentrations of Nd and I, respectively. (**e**) *In vivo* X-ray bioimaging of a Kunming mouse without injection (left) and subcutaneous injection (right) of Nd-DTPA. The injection site was marked with blue-dotted lines. The injected site with Nd-DTPA showed significant X-ray absorption contrast by using *in vivo* imaging system (Bruker In Vivo FX PRO) under 45 kVp voltage.

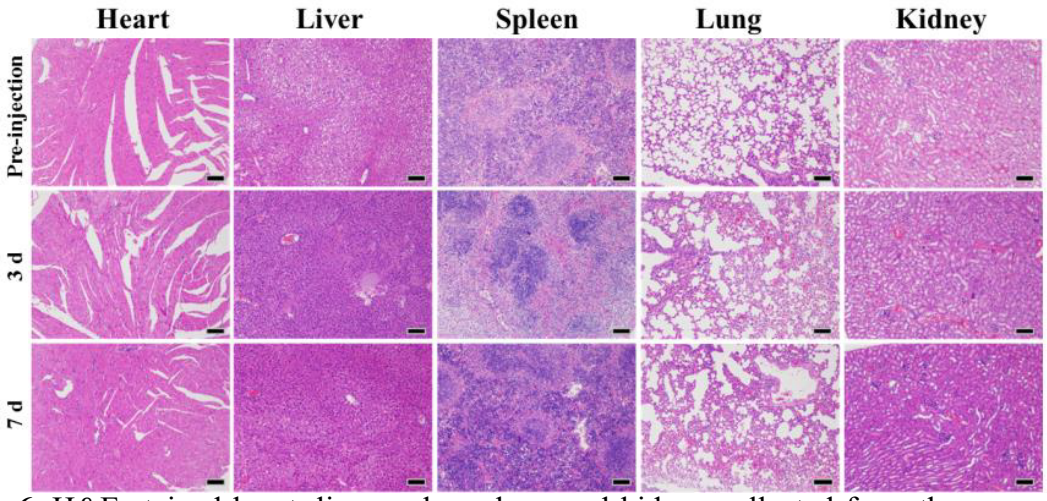

Figure 6. H&E stained heart, liver, spleen, lung and kidney collected from the mouse with injection of Nd-DTPA and control group without injection were analyzed. The isolated tissues present no obvious damage. All the scale bars are 100 μm.

A new type of molecular NIR-II-emitting probe based on Nd-DTPA was developed. This Nd-based complex presents high biocompatibility, rapid renal excretion and narrow-band emission at 1330 nm for highly sensitive NIR-IIa bioimaging and tiny tumor detection. These findings open up the possibility for designing a new generation of multi-modal small molecular probe for early tumor diagnosis and favor the clinic translation of the advanced NIR-II imaging method.

Keywords: molecule probe, NIR-II bioimaging, renal clearance, tiny tumor diagnosis, X-ray bioimaging.

Youbin Li, Xiaolong Li, Zhenluan Xue, Mingyang Jiang, Songjun Zeng, and Jianhua Hao**

Second near-infrared emissive lanthanide complex for fast renal-clearable *in vivo* optical bioimaging and tiny tumor detection

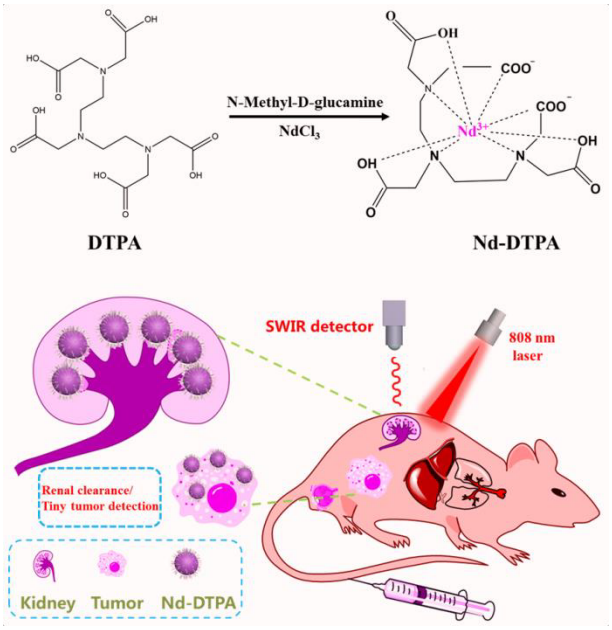

Supporting Information

Second near-infrared emissive lanthanide complex for fast renal-clearable *in vivo* optical bioimaging and tiny tumor detection

Youbin Li, Xiaolong Li, Zhenluan Xue, Mingyang Jiang, Songjun Zeng, and Jianhua Hao**

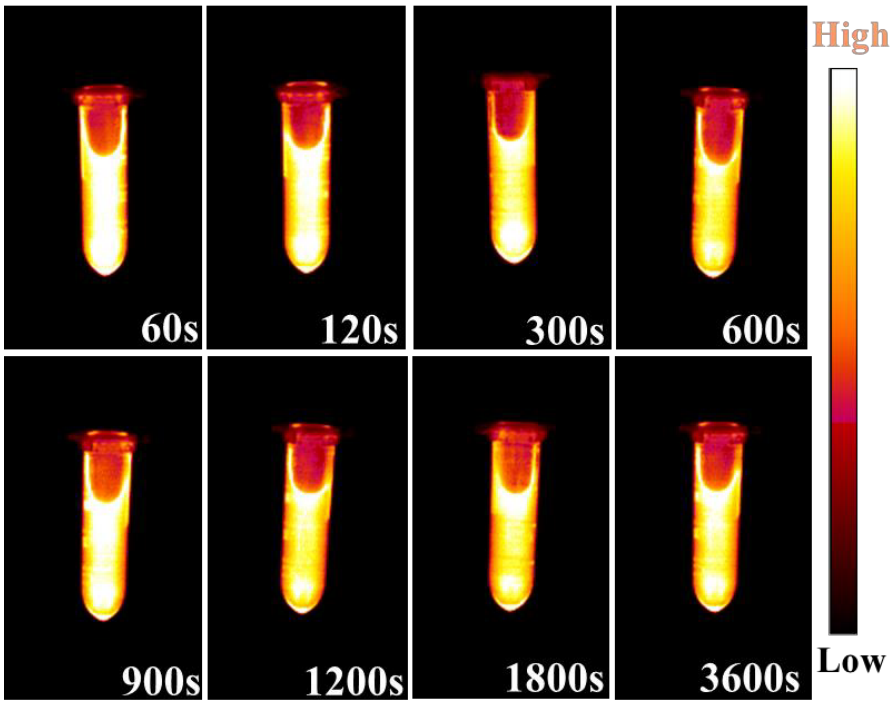

Figure S1. The pictures show the NIR-II fluorescence images of Nd-DTPA under continuous 808 nm excitation with an output power density of 1w cm^{-2} at different period times. The fluorescence signal was collected by using the *in vivo* NIR-II bioimaging system.

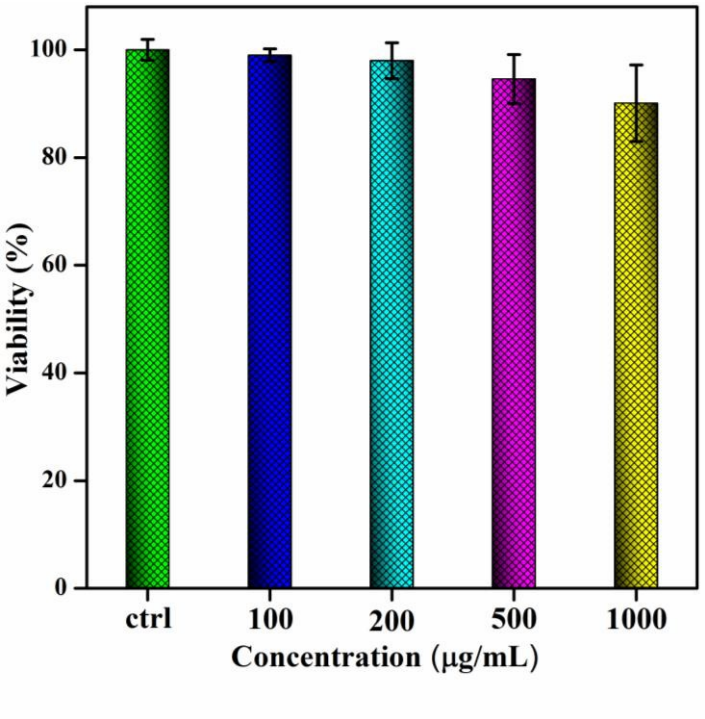

Figure S2. The cell toxicity of HeLa cells treated with different concentrations of Nd-DTPA at 37 C for 24 h under 5% CO_2. The result indicated the very low cell toxicity of Nd-DTPA molecules.

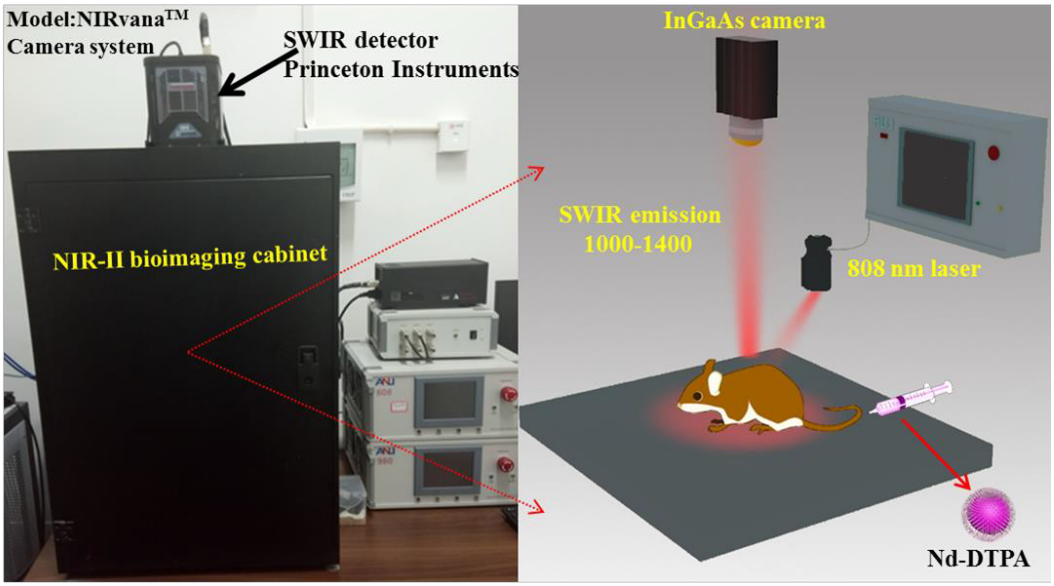

Figure S3. The NIR-II imaging system consists of a highly sensitive InGaAs SWIR detector (Model: NIRvana™ Camera System, Default Operating temperature: -80 ℃, Princeton Instruments), the fiber-coupled 808/980 nm laser with tunable power density from 0-100 mW/cm^2 and an optical bioimaging dark cabinet. The 808 nm laser was used as excitation light resource in this work. Efficient fluorescence signal in the second near infrared window (1000-1700 nm) can be captured by the SWIR detector.